

## Electronic structure and properties of *d*- and *f*-shell-metal compounds

Walter A. Harrison

*Department of Applied Physics, Stanford University, Stanford, California 94305*

Galen K. Straub

*Los Alamos National Laboratory, University of California, Los Alamos, New Mexico 87545*

(Received 21 January 1987)

Bonding in rock-salt-structure compounds is described. For NaCl, the bonding is in terms of electrons occupying chlorine *p* bands, lowered in energy by interaction with the sodium *s* states, and an overlap repulsion arises from nonorthogonality of states on neighboring ions. For transition-metal compounds *d*-like states are added, with their coupling with the nonmetallic *p* states. This coupling is taken to be of the form  $\eta_{pdm} \hbar^2 (r_p r_d^3)^{1/2} / (md^4)$ , with  $r_p$  and  $r_d$  tabulated for each element. An additional overlap repulsion, proportional to  $\hbar^2 r_p r_d^3 / (md^6)$  and to the number of electrons occupying the corresponding bands, also arises from this interaction. The simplest systems, such as KF, CaO, ScN, and TiC, contain eight valence electrons per atom pair and all but TiC are insulating. The extra energy from the covalent *pd* coupling is calculated; it decreases the lattice distance and increases the cohesion and bulk modulus. With a total valence of 9–12, the excess electrons occupy nonbonding bands making the compound metallic, but not significantly modifying the bonding properties. A total valence of 13–18 would require electrons in antibonding bands and such compounds appear not to occur in the rock-salt structure unless intra-atomic Coulomb interactions are strong enough (as in the heavy-3*d*-metal compounds) to produce a correlated state, insulating, magnetic, and with suppressed covalent interactions. The form of the condition for the formation of a correlated state is written. This same general theory is applied also to *f*-shell compounds, those of the rare earths and actinides, with *pf* coupling proportional to  $\hbar^2 (r_p r_f^3)^{1/2} / (md^5)$  replacing the *pd* coupling of the transition-metal compounds. The theory suggests that a correlated state of the *f* electrons may be expected except for cerium compounds and compounds of the light actinides. The phosphides of the actinides are predicted to, and found to, have minimum spacing at the uranium phosphide which occurs as the metal *f* level drops below the nonmetal *p* level; the effect is less pronounced experimentally in the nitrides, arsenides, and sulphides. The contribution of the *pf* bonding to the cohesion increases through the series as long as the *f* levels do not form correlated states.

### I. INTRODUCTION

The electronic structure of alkali halides, and of the divalent counterparts in the rock-salt structure, is easily understood in terms of closed-shell ions. The qualitative electrical, dielectric, magnetic, and bonding properties are immediately understandable and can be predicted using tight-binding theory and universal tight-binding parameters.<sup>1,2</sup> Once the alkali metal is replaced by a transition metal, a wide diversity of properties arises, reflecting a diversity of basic electronic structure. A considerable variety of theoretical analyses<sup>3–6</sup> have clarified the nature and variety of this electronic structure, and some of the properties. There seems to be no simple coherent theory which allows us to understand simply and predict the variety of behavior. We seek here to provide such a theory.

In order to focus on a coherent set of systems, we discuss only *AB* compounds, meaning equal numbers of ion type *A* and ion type *B*, and only the rock-salt structure. The valence of a metal shall refer to the column number of the element, one for K, two for Ca, increasing by one each step through the transition-metal series to nickel, of valence ten. We shall also consider metals in the

lanthanide and actinide series. Nonmetals from columns 4, 5, 6, and 7 (e.g., C, N, O, and F) will be considered. The principal concepts and formulas introduced are clearly applicable to other systems and other structures, but it will be better to limit the discussion here.

We begin with the tight-binding theory of alkali halides, and extend it step by step to other systems, discussing in each case the electronic structure and the basic properties of each system. The principal formulas needed are for the various contributions to the energy, each written in terms of tight-binding parameters of the system. These are quoted and either sources or derivations are given in Appendices to this paper. Given these formulas, and the parameters of the system, the variety of properties may be directly predicted. The accuracy is low, but is sufficient to show correctly the variety of contrasts and trends among these systems.

### II. SIMPLE-METAL COMPOUNDS

In the alkali halide the alkali gives up its valence *s* electron to the halogen valence *p* shell, each atom then having closed shells of electrons. The lowest empty state, the sodium 3*s* state, has an energy (which we take to be the

Hartree-Fock free-atom term value<sup>7</sup>) of  $-4.95$  eV,  $8.83$  eV above the energy of the highest occupied state, the chlorine  $2p$  state with energy of  $-13.78$  eV. This predicted gap (closer to the observed gap of  $8.5$  eV than in most of the alkali halides) guarantees the insulating electrical behavior and the optical transparency of rock salt. The energy gain in the formation, also  $8.83$  eV from the electron transfer, is of the order of the observed cohesive energy of  $6.8$  eV per atom pair.

In tight-binding theory the forces holding the atoms together arise from the coupling between the occupied chlorine  $p$  states and the empty sodium  $s$  states. The coupling is given by a universal form in terms of the internuclear distance  $d$  as<sup>8</sup>  $V_{sp\sigma} = -1.42\hbar^2/md^2$ . If calculated in perturbation theory the energy per ion pair associated with the attraction is<sup>1,2</sup>  $12V_{sp\sigma}^2/(\epsilon_p - \epsilon_s)$ . There is also a repulsion between ions arising from the nonorthogonality of the orbitals on adjacent ions. It can be taken to be of the form<sup>1</sup>

$$V_0 = \eta_0 |\epsilon_{IG}| [\hbar^2/(m\epsilon_{IG}d^2)]^4, \quad (1)$$

with  $\epsilon_{IG}$  the  $p$ -state energy of the inert-gas atom from the row in the Periodic Table from which the constituent atoms come; if the constituent atoms are from two rows, the average for the two inert-gas atoms is used.  $\eta_0$  is a dimensionless constant depending upon the row of the nonmetallic atom, adjusted to give the correct spacing for the corresponding potassium halide ( $688$  for the fluorine row,  $1163$  for the chlorine row,  $1323$  for the bromine row, and we use  $1684$  for both the iodine and astatine rows). This same form for the repulsion is used also<sup>1</sup> for the interaction between nonmetallic ions (e.g., halogen ions) which are second-nearest-neighbor ions in the crystal. Given the attractive force and this form for the repulsion, one has a rather crude first-principles theory of the entire range of bonding and dielectric properties.<sup>1,2</sup> The theory of the divalent counterpart, such as calcium oxide, is just the same, with no additional parameters except the corresponding free-atom Hartree-Fock term values from the same source.

We shall at this point define notation for this theory<sup>1</sup> which can be directly generalized to the transition-metal systems. We note first the mathematical fact that if we have three  $p$  levels on each nonmetallic ion, coupled only to a single  $s$  level on each neighboring metallic ion, two  $p$  bands become uncoupled and remain at the  $p$ -state energy; these are called *nonbonding* bands. The remaining  $p$  band becomes a broad *bonding* band and the  $s$  band becomes a broad *antibonding* band. It is this broadening of the  $p$  band from the original atomic  $p$ -state energy downward which gives the lowering in energy which we estimated above in perturbation theory. The antibonding  $s$  band which broadened upward from the  $s$ -state energy is of no consequence since it is unoccupied.

It will be desirable to obtain a more accurate expression for the average energy of the bonding band than that given by perturbation theory. In Appendix A we show that the second moment of the bonding band, measured from the average of  $\epsilon_s$  and  $\epsilon_p$ , is  $(\epsilon_s - \epsilon_p)^2/4 + nV_{sp\sigma}^2$ , with  $n$  the number of nearest neighbors. We take the average energy of the band to equal the square root of this moment. Then it is convenient to call the magnitude of the

coupling, times the square root of the number of nearest neighbors, the *covalent energy*,  $V_2$ , in this case  $V_2 = \sqrt{6}V_{sp\sigma}$ . Half the energy difference is called the *polar energy*,  $V_3$ , in this case  $V_3 = (\epsilon_s - \epsilon_p)/2$ . The average energy of the bonding band, relative to the average of  $\epsilon_s$  and  $\epsilon_p$  then becomes  $-(V_2^2 + V_3^2)^{1/2}$ . With two electrons in the bonding band this approaches the result of perturbation theory when  $V_2 \ll V_3$  and remains valid when  $V_2$  and  $V_3$  are comparable.

We shall wish to add various contributions to the total energy per ion pair. Starting from free atoms we obtained contributions to the cohesion from transferring electrons between levels, using free-atom term values. We call that  $E_{\text{trans}}$ ; it was  $-2V_3$  per atom pair for alkali halides. We separate the effect of the covalent energy as  $2V_3 - 2(V_2^2 + V_3^2)^{1/2}$  per ion pair. It approaches the perturbation-theoretic result when  $V_2$  is small. Then the contribution of the  $sp$  coupling to the total energy, including the overlap repulsion, is

$$E_{sp \text{ bond}} = 2V_3 - 2(V_2^2 + V_3^2)^{1/2} + 6V_0(d) + 6V'_0(\sqrt{2}d) \quad (2)$$

per ion pair, to be added to  $E_{\text{trans}}$ . It is a small correction to the cohesion. The final term is the repulsion between a nonmetallic ion and its twelve neighboring nonmetallic ions at a distance  $\sqrt{2}d$  away, with  $d$  again the nearest-neighbor distance. Half the energy is associated with each ion, yielding a prefactor 6. The prime indicates use of different  $\epsilon_{IG}$  if the metallic ion comes from a different row than the nonmetallic ion.

We found in Ref. 1 that there were significant Coulomb corrections to the cohesion. These arose because the extra electrons on the nonmetallic atom felt a repulsion  $U$  due to the  $Z$  excess electrons on that ion which was not entirely canceled by the Madelung potential  $-Zae^2/d$  from the neighboring ions. We found that correction to be approximately  $\frac{1}{2}Z(Z+1)U^*$ , with  $U^* = U - ae^2/d$ . These were several volts for the simple compounds and we shall estimate them here for the cohesion of the transition-metal compounds; their effects on other properties are quite small.

Given Eq. (2), the free-atom term values, and the four  $\eta_0$  listed above, we may immediately minimize the energy with respect to  $d$  to predict the equilibrium  $d$  for any monovalent or divalent compound in the rock-salt structure. We may also predict immediately the bulk modulus and Grüneisen constant and corrections to the predicted cohesive energy,  $E_{\text{trans}}$ , given above. This exercise was carried out for simple-metal compounds in Ref. 1. We have, of course, also the prediction of a large gap,  $\epsilon_s - \epsilon_p$ , giving insulating properties and could predict the dielectric and magnetic susceptibilities and other properties in terms of the same parameters, as done in Ref. 2. Our goal here is to extend this simple, but general, theory to the corresponding compounds containing transition-metal and  $f$ -shell-metal ions, using the tight-binding theory of such systems.<sup>2</sup>

### III. OCTET COMPOUNDS OF TRANSITION METALS

We begin by extending the theory to compounds which also have a total of eight valence electrons (including the

metallic *s* and *d* electrons and the nonmetallic *p* and *s* electrons). The most convenient series of these starts with the alkali halide, KF, and proceeds by increasing the atomic number of the metal by one and decreasing the atomic number of the nonmetal by one, thus holding the number of electrons fixed. The series is KF, CaO, ScN, TiC. The extension to CaO is direct, as indicated above, but Sc and Ti are transition metals, having, respectively, one and two electrons in *d* states in the free atom. We must take account of which atomic states were occupied when we subtract to estimate the cohesion as  $E_{\text{trans}}$ , but the occupied valence states in the solid are the same, full nonmetallic *p*-like bands.

The atomic *d* state is ordinarily lower in energy than the atomic *s* state in the transition metal (it is in Sc and Ti, but not in K and Ca). Thus in the transition-metal compound the conduction band becomes *d*-like and the gap is determined by the difference between the nonmetallic *p*-state energy and the free-atom metallic *d*-state energy. The gaps predicted for the four compounds by subtracting term values are 15.85, 11.40, 4.49, and  $-0.03$  eV; experimentally for the four they are 10.7 and 7.7 eV, unknown by us, and less than zero.

The five *d* levels on each metallic ion, coupled to three *p* levels on each neighboring nonmetallic ion by matrix elements of the type  $V_{pd\sigma}$  and  $V_{pd\pi}$ ,<sup>2</sup> yield two *d* bands which are uncoupled and remain at the *d*-state energy (unless we include second-neighbor coupling, discussed in

Sec. V); these are nonbonding bands, analogous to the two nonbonding *p* bands discussed in the preceding section for the *sp* system. The remaining three *d* bands become broad antibonding bands and the three *p* bands become broad bonding bands.

This is illustrated in Fig. 1 where we show the bands of CrN (not an octet compound) calculated by Papaconstantopoulos *et al.*<sup>9</sup> along with tight-binding bands corresponding to the approximations and parameters used here. Indeed the two are qualitatively similar and the positions and widths of the bands, calculated completely independently, are similar. We show there also the density of states, and integrated density of states, given by Papaconstantopoulos *et al.* The peak at the Fermi energy in CrN corresponds to our nonbonding band which we take to be a  $\delta$  function in energy; note that the integrated density of states rises from eight to twelve through that peak. The four levels, accommodating eight electrons, below that consist of the lower *s* band, which we do not consider here, and the three bonding bands. These are concentrated at some 5 V below the nonbonding band. Then the antibonding bands extend upward in energy from the nonbonding bands, in this case with no gap between the bonding and antibonding bands.

The coupling between the *d* and *p* states gives an additional attraction between neighbors and reduces the spacing significantly beyond what one would expect from the *sp*-coupling theory described above. This coupling may be characterized by a covalent energy,

$$V_2(pd) = \left[ \frac{n}{3} (V_{pd\sigma}^2 + 2V_{pd\pi}^2) \right]^{1/2} \\ = \left[ \frac{75n}{4\pi^2} \right]^{1/2} \frac{\hbar^2 (r_p r_d^3)^{1/2}}{md^4}, \quad (3)$$

(derived in Appendix A) where *n* is the number of nearest neighbors (six for the rock-salt structure) and  $r_p$  and  $r_d$  are free-atom parameters (Appendix B) characteristic of the nonmetallic and metallic constituents. The polar energy becomes

$$V_3(pd) = (\epsilon_d - \epsilon_p)/2. \quad (4)$$

If the *p* electrons were coupled only to the *d* electrons, the six bonding electrons per atom pair would contribute an energy, based again upon the second moment of the bonding band,  $-6[V_2(pd)^2 + V_3(pd)^2]^{1/2}$ , analogous to the *sp*-bonding term we gave before. We may add  $6V_3(pd)$  (assuming that  $V_3$  is positive) to this to obtain just the effect of the *pd* coupling. With this attraction of course also comes a repulsion from shift in the energy of each electron due to the nonorthogonality of the *p* and *d* states. An explicit form for this repulsion, proportional to  $1/d^6$ , is obtained in Appendix C. Adding it for the six occupied bonds gives the total effect of the *pd* coupling,

$$E_{pd \text{ bond}} = 6V_3(pd) - 6[V_2(pd)^2 + V_3(pd)^2]^{1/2} \\ + \frac{45n\hbar^2 r_p r_d^3}{2\pi^2 m d^6}. \quad (5)$$

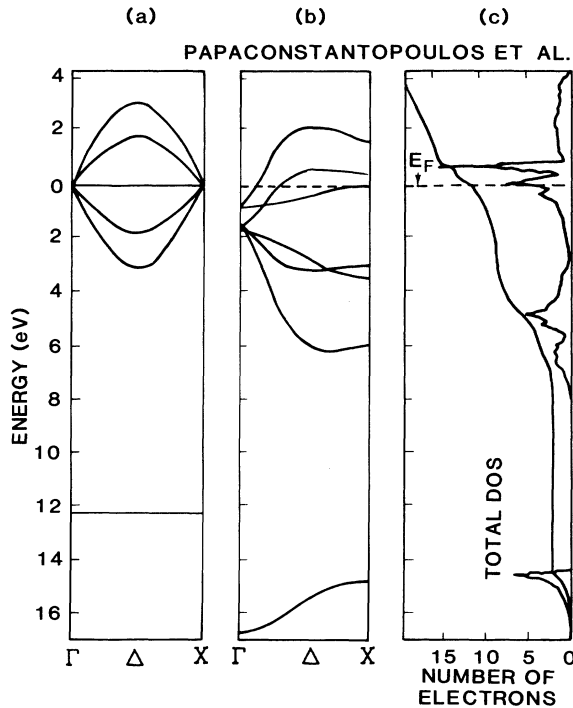


FIG. 1. The electronic energy bands of CrN. (a) Tight-binding energy bands for first nearest neighbors only, (b) the self-consistent augmented-plane-wave bands, and (c) the density of states (DOS) of Papaconstantopoulos *et al.* (Ref. 9).

TABLE I. Contributions to the cohesive energy for the octet compounds of the transition metals.

	KF	CaO	ScN	TiC
$E_{\text{trans}}(sp)$	-15.9	-22.9	-16.2	-10.1
$E_{\text{trans}}(dp)$			-4.5	-0.1
$E_{sp \text{ bond}}$	-0.9	-1.4	-1.4	-1.3
$E_{pd \text{ bond}}$			-2.1	-12.6
Total $E_{\text{trans}} + E_{\text{bond}}$	-16.7	-23.4	-24.3	-24.0
(Experiment)	(-7.6)	(-11.0)		(-14.6)
Coulomb corrections:	$U^* = 6.3$	$3U^* = 13.8$	$6U^* = 10.5$	$10U^* = 0.9$

It is to be added to the  $E_{\text{trans}}$  and  $E_{sp \text{ bond}}$  for the transition-metal compounds with a total of eight valence electrons. [This form is valid even if  $V_3(pd)$  is negative; it then includes what may formally be regarded as an energy gain in transferring electrons from the nonmetal  $p$  states to the metal  $d$  states.] We can then directly predict the bonding properties of any of these systems.  $E_{pd \text{ bond}}$  reduces the predicted spacing and increases the cohesion of these systems.

In Table I we give  $E_{\text{trans}}$  and  $E_{\text{trans}} + E_{sp \text{ bond}}$  for KF, CaO, ScN, and TiC, as well as the estimate including  $E_{pd \text{ bond}}$  for the transition-metal compounds, and the experimental cohesive energy. For these compounds with nonmetals from the first row we overestimate the cohesion by a factor of about 2 even for KF and CaO, mainly because of a large Coulomb correction which is much smaller for compounds in which the nonmetal is from a lower row.<sup>1</sup> As indicated in Sec. II, this correction is given by a net Coulomb repulsion  $U^*$  times  $\frac{1}{2}Z(Z+1)$ , with  $Z$  the number of electrons transferred in the step leading to  $E_{\text{trans}}$ .<sup>1</sup>  $U^*$  drops with increasing  $Z$ , being near zero for TiC, while the  $Z(Z+1)$  factor is growing rapidly making the correction very sensitive to the approximations made. The correction is included as one entry in Table I, im-

proving the agreement with experiment, but still leaving it only semiquantitative. This correction would be much smaller for octet compounds of the transition metals with the heavier nonmetals but there are almost no such compounds with which to compare.

In Fig. 2 we show the predicted internuclear distances, and the experimental values, for this series. (For these calculations the effect of the Coulomb corrections is small and they are not included.) We also show the predictions for the transition-metal compounds neglecting the effect of  $E_{pd \text{ bond}}$ . The additional pressure due to  $E_{pd \text{ bond}}$  has given approximately the correct lattice contraction for ScN and TiO. Our overestimate of the spacing in CaO would suggest some effect of the  $pd$  coupling in that system, and possibly even in KF. However, with the calcium, or potassium,  $d$  level well above the  $s$  level, it seems unlikely that our transition-metal parameters apply. We conclude that the simple-compound theory makes errors by ignoring the  $d$  states already in CaO, but that our transition-metal theory has not yet become appropriate.

#### IV. VARIATION WITH ROW OF METAL OR NONMETAL

Elements of the same column in the Periodic Table are chemically equivalent so one does not expect qualitative differences when the row number of either constituent is changed, and this is true. Thus we could talk about NaCl and KF with the same outlook, but using different atomic term values. Similarly we may use the same formulas as given above when ScN is replaced by YN, LaN, or AcN. The repulsion is larger for metals lower in the Periodic Table, due here to the smaller  $\epsilon_{IG}$  in  $V_0$ , and the spacings are larger. The effect is larger when the nonmetallic ion is changed, as from LaN to LaP, because of the different  $\eta_0$  as well as the different  $\epsilon_{IG}$ . We noted also in Sec. III that very few octet compounds with heavier nonmetals exist in the rock-salt structure; this may be related to the larger equilibrium spacing they would have if they existed.

#### V. NONBONDING ENERGY BANDS, 9-12 ELECTRONS

In Sec. III we let the column of the two constituents vary such that the number of electrons remained fixed at eight. We now fix the nonmetal, say nitrogen, and let the metallic ion change from Sc to Ti to V to Cr to Mn, etc., adding an electron at each step. Similarly we could hold

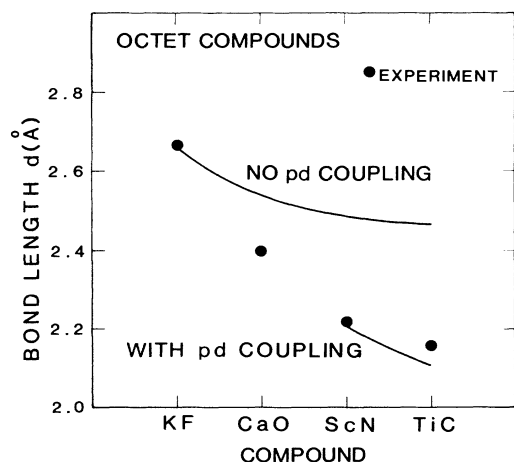


FIG. 2. The bond lengths for the octet compound series KF, CaO, ScN, and TiC. The upper curve is the bond-length prediction without  $pd$  coupling and the lower curve includes  $pd$  coupling. The solid points are experimental values.

TABLE II. The predicted cohesive energy, bond length, and bulk modulus of the 3*d*-transition metal nitrides. Energies are in eV and the bulk modulus is in Mbars. The Coulomb corrections to the cohesive energy are given by  $6U^* = 6(U - \alpha e^2/d)$ , where  $U = 13.15$  eV for nitrogen and the experimental value of  $d$  was used.

	ScN	TiN	VN	CrN	MnN
$V_2(sp)$	5.44	5.99	6.23	6.30	6.20
$V_2(pd)$	3.44	3.39	3.18	2.86	2.59
$E_{\text{trans}}(sp) = -4V_3(sp)$	-16.24	-15.6	-15.04	-14.5	-14.0
$E_{\text{trans}}(pd) = -2V_3(pd)$	-4.49	-2.8	-0.13	0.10	1.43
$E_{\text{bond}}(sp)$	-1.44	-0.59	-0.11	-0.05	-0.45
$E_{\text{bond}}(pd)$	-2.09	-5.59	-8.81	-12.03	-15.89
Total ( $E_{\text{trans}} + E_{\text{bond}}$ )	-24.3	-24.6	-24.05	-26.5	-28.93
$E_{\text{coh}}$ (Experiment)		-12.9	-12.	-10.3	
Coulomb corrections: $6U^*$	10.8	7.2	7.2	7.2	
Predicted bond length $d$	2.21	2.10	2.06	2.05	2.07
(Experiment)	(2.22)	(2.11)	(2.11)	(2.11)	
Predicted bulk modulus	1.46	2.57	3.27	3.39	2.89

the metallic column fixed and change the column of the nonmetallic ion, as from LaP to LaS. (We did not use ScN to ScO as an example since the latter does not exist in nature.) Taking a nonmetal of one higher valence increases the electron count by one, just as does increasing the valence of the metal. The valence bands are already full so the extra electrons must be accommodated in the *d*-like nonbonding conduction bands, those levels which become uncoupled as indicated in Sec. III.

Indeed now we can accommodate the first four extra electrons from the transition metals to the right of scandium in the nonbonding band in the nitride and they do not contribute to the bonding of the compound. Thus the change in column is of no consequence up through MnN or the oxide FeO, with a total of 12 valence electrons and Eq. (5) remains appropriate. The repulsive interaction between atoms also depends upon which states are occupied, but is proportional to the coupling (as well as to the nonorthogonality of the states) and vanishes for the nonbonding bands. Thus again the additional electrons are not of consequence to the bonding.

There are of course minor changes arising because the atomic parameters for each element are a little different.<sup>10</sup> These in fact give a small steady decrease in spacing with increased valence of the metal, as illustrated for 3*d* nitrides in Fig. 3 and in Table II. There is an even more substantial decrease in spacing with increased valence of the nonmetal.

Again the predicted cohesion, listed in Table II, is too large by a factor of about 2. The *pd* bonding makes again a significant contribution to the cohesion, and that of course only increased the discrepancy. The predicted bulk moduli also appear in Table II; we did not find corresponding experimental values, but found in our earlier study of the simple-metal compounds<sup>1</sup> that we underestimated them considerably.

One of the changes due to an increase in the valence of the metal is the lowering of the *d*-state energy in comparison to the nonmetallic *p*-state energy until (near CrN, for example)  $V_3(pd)$  goes through zero and then the *d* state lies below the *p* state. Then the nonbonding *d* band lies at

the top of the valence band, rather than at the bottom of the conduction band. The same formulas for the contribution to the total energy given above still apply, as we indicated after Eq. (5).

The representation of the nonbonding band as flat is only approximate, and came from the inclusion of nearest-neighbor coupling only. Complete band calculations, such as those shown in Fig. 1 for CrN, indicate an overlapping of the bands and a broadening of the nonbonding band. The principal source of this broadening is the coupling between neighboring *d* states, second-neighbor atoms in the crystal. It is thus much smaller than the width in energy of the bonding band (and also the antibonding band). The latter can be obtained from

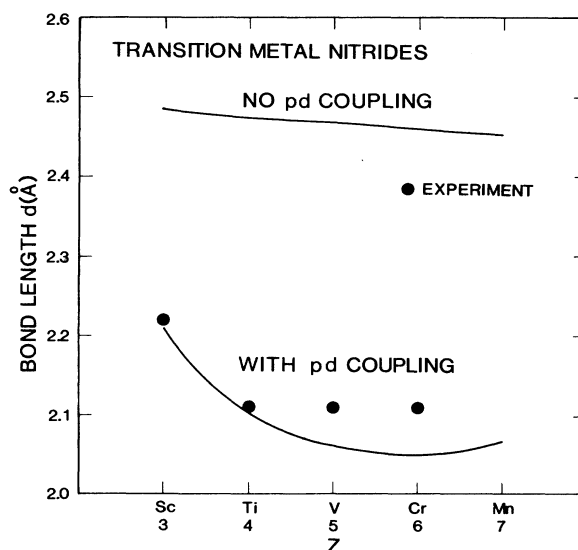


FIG. 3. The bond lengths for the transition-metal nitride compounds. The upper curve is the bond-length prediction without *pd* coupling and the lower curve includes *pd* coupling.  $Z$  is the total number of valence electrons on the metallic ion.

Eq. (A6) in Appendix A; when  $V_3(pd) \ll V_2(pd)$ , which is usually the case, it reduces to

$$W_b \approx 2V_2(pd). \quad (6)$$

The nonbonding band width, arising from the coupling between neighboring  $d$  states, is found to be

$$W_d(\text{nonbond}) = 11.98\hbar^2 r_d^3 / (md^5)$$

[obtained as was Eq. (B4) for  $p$  bands] equal to 1.75 eV for CrN. This is smaller than the width of the bonding band by a factor of approximately  $(r_d^3/d^2r_p)^{1/2}$ , equal to 0.18 for CrN. The partial occupation of these bands gives an additional pressure, an energy per atom pair given by  $\frac{1}{2}Z_{\text{NB}}(1 - Z_{\text{NB}}/4)W_d(\text{nonbond})$ , which would reduce the lattice spacing but the effect is small enough that we have neglected it here. We also then neglect the additional second-neighbor repulsion which arises from this coupling.

An important effect of the electrons in the nonbonding band is that they do provide a partially filled band and metallic conductivity to the compound. This is a major change in the electrical and optical properties. Because these nonbonding bands are narrow, and the density of states at the Fermi energy is therefore high, we may expect these systems to be superconductors with moderately high critical temperatures.

Experimentally CrN is antiferromagnetic. This would appear to be the result of an instability against spin-density-wave formation of the three electrons per atom occupying the nonbonding bands, and not a fundamental change in electronic structure such as we describe in the following section.

## VI. THE CORRELATED STATE, 13–18 ELECTRONS

Let us proceed tentatively as above to FeN or MnO, with 13 electrons, and put the additional electron in the antibonding band. This would be energetically unfavorable; the bond length would be expanded and the cohesion would be reduced, both by the excess energy of the electron in the nonbonding band and the extra overlap repulsion associated with the antibonding band. Indeed there are essentially no  $AB$  compounds in the rock-salt structure composed of one transition-metal ion from the  $4d$  and  $5d$  rows and one nonmetal ion, such that the total number of valence electrons is 13–18. The reason is certainly the destabilization due to the antibonding electrons. There are a number of  $AB$  compounds of  $4d$  and  $5d$  metals in more complicated structures with partly filled bands,<sup>5</sup> but in these structures the antibonding character may be less clear. The corresponding rock-salt-structure compounds do, however, form for the  $3d$  transition metals.

For compounds of the high-valent  $3d$  metals, Cr, Mn, Fe, Co, and Ni, a new effect arises which is ordinarily associated with magnetic behavior, though in some sense the magnetism is incidental. Whenever two electronic levels are sufficiently weakly coupled, as when two hydrogen atoms are spaced widely apart, it becomes energetically favorable for each electron to reside on one atom, avoiding the Coulomb repulsion of the other, rather than for

the two to occupy bond states in which they inevitably may be found at some moment on the same atom. This is the so-called Heitler-London transition. The resulting state is frequently called a *localized* state, though we prefer the term *correlated* state. The real state in either case is more complicated but the two concepts represent different starting points for calculation of the state or different appropriate physical pictures. When the correlated state is formed we no longer think of bonding, nonbonding, and antibonding states and the excess electrons no longer inhibit the formation of the compound. Correspondingly, the necessity of placing electrons in nonbonding states in compounds with 13 or more electrons favors the formation of the correlated state.

We analyzed such a system, weakly coupled  $f$  levels in a pure  $f$ -shell metal, using the unrestricted Hartree-Fock approximation.<sup>11</sup> We found the condition for the formation of a correlated state was that a resonance width, equal to 0.677 times the band width, must be less than  $2U/\pi$  times a function of occupation,  $\sin^2(Z_f\pi/14)$  with a fraction  $Z_f/14$  of the  $f$  states occupied.  $U$  is an intratomic Coulomb repulsion, equal to the change in energy of an  $f$  state when an electron is transferred from an  $s$  to an  $f$  state in the free atom. We might say that if this criterion is satisfied [that is,  $W_f < 0.94U \sin^2(Z_f\pi/14)$ ], the system may best be described as having formed a correlated state. We also found that the bonding energy due to the coupling is reduced by a factor of  $W_f/6U$  (in the unrestricted Hartree-Fock approximation) when this correlated state is formed.

Such a criterion is more difficult to construct for the compound. The width of the bonding band, determined in the present case by  $V_2(pd)$ , is relevant since it determines the energy gain from bond formation. Again the atomic  $d$  state  $U$ , tabulated by Froyen,<sup>12</sup> represents quantitatively the tendency for the state to become correlated. We expect the correlated state to be established when  $U$  becomes sufficiently large in comparison to  $V_2(pd)$ . We may also expect a counterpart,  $\sin^2(Z_d\pi/10)$ , of the factor depending upon filling of the level to apply, but we have not derived the dividing point. We can however evaluate  $V_2(pd)$  from Eq. (3) for the monoxides from TiO to NiO, for which we have empirical values for  $d$ . These drop from 9.3 to 4.3 eV through the series. The values of  $U$  for these metals, given by Froyen,<sup>9</sup> rise from 3.7 to 5.7 eV through the same series and may be multiplied by  $\sin^2(Z_d\pi/10)$ . Indeed  $U \sin^2(Z_d\pi/10)$  first rises above  $V_2(pd)$  at the compounds MnO, where there are 13 electrons. If we assert that such compounds will be stable only if the correlated state occurs, we conclude that a *correlated state occurs when  $U \sin^2(Z_d\pi/10)$  exceeds  $V_2(pd)$  for the compound*. In fact  $\sin^2(Z_d\pi/10)U$  exceeds  $V_2(pd)$  also for FeO, but drops below again for CoO and NiO, though the observed bond lengths, and insulating behavior, would indicate that the entire set of compounds have correlated states. We may count this as an incorrect prediction for CoO and NiO.

The same evaluation for the nitrides ScN through CrN gives  $V_2(pd)$  values more than twice  $\sin^2(Z_d\pi/10)U$ , with band states expected. All rock-salt-structure compounds with the  $4d$ - and  $5d$ -transition metals had larger  $V_2(pd)$

and smaller  $U$  and were far from forming correlated states.

When the correlated state appears, each  $d$  electron becomes associated with a single ion. The correlated state will ordinarily be insulating or semiconducting, with various mechanisms for conduction being possible, as discussed by Zaanen, Sawatzky, and Allen.<sup>5</sup> The spins on each ion align, according to Hund's rule, giving a spin per ion equal to one-half the number of electrons in  $d$  states,  $\frac{3}{2}$  for CrN. This is an indication of the formation of the correlated state, though the gain in energy from spin alignment is small and is not the driving force for the formation of the state. It is the same driving force which produced the antiferromagnetic state in CrN, in that case presumably without destroying the bands.

## VII. RARE-EARTH COMPOUNDS

Lanthanum, the last element before the rare-earth series, contains two valence  $s$  electrons and one valence  $d$  electron. It is thus electronically the same as scandium, discussed above. It forms compounds with elements of the same valence as nitrogen, and also nonmetals of higher valence. We focus here on the nitrides. The  $d$  band in LaN is empty but its interaction with the nitrogen  $p$  bands decreases the internuclear distance and enhances the cohesion according to Eq. (5). The compound is insulating and nonmagnetic.

Moving in the Periodic Table to the right from lanthanum, the free atom contains successively additional valence electrons in  $f$  states. We must then consider the  $f$  states interacting with the nonmetallic  $p$  states just as we considered the  $d$  states interacting with the nonmetallic  $p$  states above. In fact the Coulomb  $U$  for rare-earth  $f$  states is large, varying from 5 to 8 eV through the series.<sup>11</sup> The counterpart for  $pf$  coupling of Eq. (3) is

$$V_2(pf) = \left[ \frac{n(V_{pf\sigma}^2 + 2V_{pf\pi}^2)}{3} \right]^{1/2} \\ = \left[ \frac{1225n}{\pi^2} \right]^{1/2} \frac{\hbar^2(r_p r_f^5)^{1/2}}{md^5} \quad (7)$$

The largest value of  $V_2(pf)$  (taking  $r_p$  from Appendix B and  $r_f$  from Ref. 19) is for CeN, 0.69 eV and with  $Z_f = 1$ , the quantity  $U \sin^2(Z_f \pi / 14)$  is 0.28 eV, less than  $V_2(pf)$ . We correctly predict that only for CeN will bands be formed. Except for this one case, we expect a correlated state of the  $f$  electrons to be formed, removing their contribution to the bonding, and leaving the properties of the compound almost identical to those of the lanthanum compound. However, they have a local magnetic moment on each atom, increasing by one-half unit at each step beyond lanthanum until the shell is half full and then dropping by one-half unit to the end of the series, with some minor irregularities.<sup>13</sup> One of these irregularities gives ytterbium a  $Z_f$  of 14 rather than 13. Otherwise we would have predicted an uncorrelated state for YbN as well as CeN.

Experimentally the bonding and magnetic properties indicate that all do form correlated states except for

CeN, for which we have indeed found that  $U \sin^2(Z_f \pi / 14) < V_2(pf)$ . Cerium, the nearest neighbor to lanthanum, is also the only rare earth to form  $f$  bands rather than a correlated state as a pure metal (actually at low temperature). We postpone a quantitative analysis of the effects of  $fp$  bonding to the next section.

The extra electron in this nine-electron compound, CeN, is placed in a nonbonding band. The coupling between the  $f$  levels and the nonmetal  $p$  bands decreases the spacing and enhances the cohesion. We might expect a similar contraction in CeO, which would differ only by the addition of a nonbonding electron, but CeO appears not to exist in the rock-salt structure. If nitrogen is replaced by the larger phosphorus or any other element from the lower rows in the Periodic Table, the increased spacing decreases the coupling and it is not surprising that all form correlated states as in the rare-earth nitrides (with the exception of CeN).

## VIII. ACTINIDE COMPOUNDS

The actinides are the  $5f$  series, analogous to the  $4f$  series of rare earths. AcN is the direct analogue of ScN and LaN. In order to see if the  $f$  levels form correlated states or bands we may evaluate the covalent energy  $V_2(pf)$  for the series of actinide nitrides from Eq. (7). We use the observed spacing  $d$  and obtain values which are listed in Table III for the phosphides, arsenides, and sulfides, as well as for the nitrides; these are also plotted in Fig. 4. The values of  $U \sin^2(Z_f \pi / 14)$  are the same for all of these compounds and are also plotted in Fig. 4. We

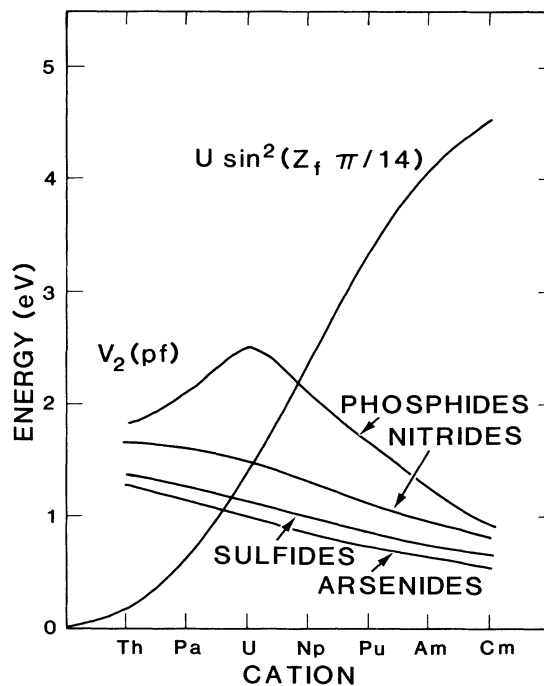


FIG. 4. A comparison of  $U \sin^2(Z_f \pi / 14)$  and the  $pf$  coupling energy  $V_2(pf)$  for the actinide phosphides, nitrides, sulfides, and arsenides.  $V_2(pf)$  is evaluated at the experimental value of the bond length for the compounds.

TABLE III. Parameters determining the formation of a correlated  $f$  state in the actinide compounds. All energies are in eV. The  $U$  values for the actinides were calculated from Hartree-Fock theory with relativistic corrections [see R. D. Cowan, *The Theory of Atomic Structure and Spectra* (University of California Press, Berkeley, 1981)].  $V_2(pf)$  is calculated at the experimental value of the bond length.

	$\epsilon_f$	$U$	$U \sin^2(Z_f \pi/14)$	N	$V_2(pf)$		
					P	As	S
Th	-7.06	3.11	0.15	1.65	1.85	1.27	1.38
Pa	-8.67	3.32	0.63	2.33	1.99	1.66	0.88
U	-10.09	3.56	1.38	1.48	2.51	1.00	1.14
Np	-11.41	3.80	2.32	1.27	2.09	0.83	0.98
Pu	-12.64	4.03	3.27	1.16	1.70	0.75	0.86
Am	-13.81	4.26	4.05	0.95	1.24	0.67	0.75
Cm	-14.96	4.51	4.51	0.81	0.96	0.57	0.66

see that  $V_2(pf)$  is less than  $U \sin^2(Z_f \pi/14)$  at the beginning of the series, crossing the nitride line between uranium and neptunium, suggesting that  $f$  bands should form for ThN, PaN, and UN. The crossing occurs further to the left for the other compounds, but in all cases the comparison suggests that bands form at the beginning of the series but not further to the right. The formation of  $f$  bands in the actinides, but not the lanthanides, corresponds to the trend noted earlier that the heavier transition elements, because of their small  $U$ 's, do not have the same tendency to form localized states in the metal as do those in the  $4f$  series. In fact it is generally believed<sup>11</sup> that of the actinide *metals*, thorium through plutonium have  $f$  bands but beyond that they do not. Our analysis of the interatomic spacing will suggest that bands occur further to the right in these series than the crossings in Fig. 4 would indicate. Thus our prediction of which systems form bands, based upon the criterion developed in Sec. VI for transition-metal oxides, was only qualitatively valid for the nitrides of the actinide metals.

It is appropriate to proceed with a discussion of the  $pf$  contribution to the bonding for the actinides at the beginning of the series, and for cerium. The contribution to the bonding from the lowering of the filled nonmetallic  $p$  band, analogous to Eq. (5), is

$$E_{pf \text{ bond}} = 6V_3(pf) - 6[V_2(pf)^2 + V_3(pf)^2]^{1/2} + \frac{1050n\hbar^2 r_p r_f^5}{\pi^2 m d^8} \quad (8)$$

per atom pair. As we proceed across the series in which  $f$  bands exist, we add electrons to the lower conduction bands which are nonbonding  $d$  bands or nonbonding  $f$  bands with little expected effect upon the cohesion or upon the bond length. The contribution from Eq. (8) reduces the spacing for all compounds. In Fig. 5 we have plotted the predicted spacing for the phosphides with and without the effects of  $pf$  coupling. The fact that the experimental values lie near the prediction which included  $pf$  coupling suggests that bands form further to the right than suggested by our comparison of  $V_2(pf)$  and  $U \sin^2(Z_f \pi/14)$  in Fig. 4. Plots of the nitrides, arsenides, and sulphides lead to the same conclusion. Since even with  $pf$  coupling we predict an increase in the spacing to the right of uranium phosphide, we cannot tell

whether the observed experimental increase arises from this effect of the bands or from a formation of a correlated state.

It is somewhat of a surprise that the spacing has a minimum in this series since  $E_{sp \text{ bond}}(d)$  from Eq. (2) is almost the same for all compounds of the same nonmetal and  $r_f$  decreases steadily with increasing atomic number. Thus we might expect the effect of the  $pf$  coupling to decrease steadily across the series, giving an increasing  $d$  with increasing atomic number. In fact  $V_3(pf)$  is found to go through zero in each series as the  $f$  level drops below the  $p$  level of the nonmetallic atom. The attraction  $\partial E_{pf \text{ bond}}/\partial d$  from Eq. (8) is dominated by the term

$$-6 \frac{\partial [V_2(pf)^2 + V_3(pf)^2]^{1/2}}{\partial d} = -6 \frac{V_2(pf)}{[V_2(pf)^2 + V_3(pf)^2]^{1/2}} \frac{\partial V_2(pf)}{\partial d} \quad (9)$$

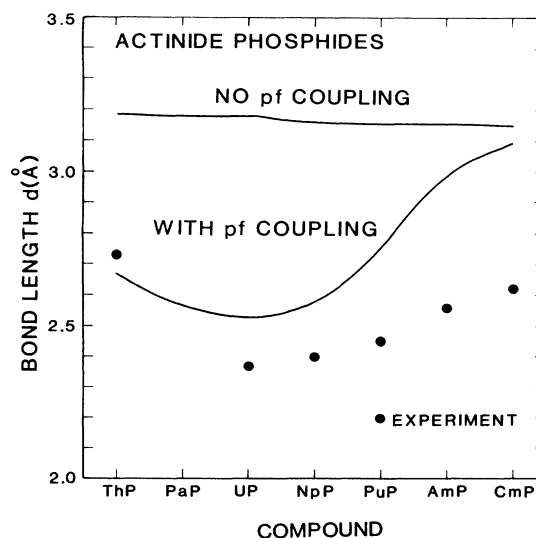


FIG. 5. The bond lengths for the actinide phosphide compounds. The upper curve is the bond-length prediction without  $pf$  coupling and the lower curve includes  $pf$  coupling. The experimental points are taken from Ref. 6.



TABLE IV. The parameters and predicted bond length  $d$ , cohesive energy, and bulk modulus of the actinide arsenide series of compounds. All energies are in eV and distances in Å; the bulk modulus is in Mbars. The Coulomb correction  $U^*$  is zero for the entire series of arsenides.

Compound	ThAs	PaAs	UAs	NpAs	PuAs	AmAs	CmAs
$d_{\min}$ (experiment)	2.82 (2.98)	2.71	2.69	2.81 (2.92)	3.12 (2.93)	3.25 (2.94)	3.29 (2.95)
$V_3(sp)$	1.85	1.80	1.75	1.70	1.66	1.61	1.57
$V_3(pd)$	1.99	1.95	1.93	1.94	1.96	1.98	2.01
$V_3(pf)$	1.48	0.69	-0.02	-0.67	-1.29	-1.87	-2.44
$V_2(sp)$	3.34	3.62	3.67	3.36	2.73	2.51	2.45
$V_2(pf)$	1.70	1.66	1.44	1.02	0.55	0.41	0.33
$E_{\text{trans}}(sp)$	-7.40	-7.20	-7.00	-6.82	-6.62	-6.44	-6.26
$E_{\text{trans}}(pd)$	-3.99	-3.90	-3.87	-3.88	-3.91	-3.96	-4.03
$E_{sp \text{ bond}}$	-0.24	0.61	0.74	-0.36	-1.43	-1.57	-1.62
$E_{pf \text{ bond}}$	-2.07	-4.39	-7.10	-10.47	-15.82	-22.57	-29.28
$E_{\text{coh}}$	-13.70	-14.87	-17.23	-21.52	-27.78	-34.53	-41.19
<b>B (Mbars)</b>	0.39	0.80	0.93	0.42	0.13	0.11	0.11

and the ratio  $V_2(pf)/[V_2(pf)^2 + V_3(pf)^2]^{1/2}$ , analogous to the covalency defined for  $sp$ -bonded systems, is maximum when  $V_3(pf)$  is zero. This turns out to be the dominant effect, giving the strongest attraction when this covalency is unity.

The experimental minimum is most pronounced for the phosphides and almost nonexistent for the arsenides. Nevertheless we may illustrate the effect using the theoretical values for the arsenide series. In Table IV we give the relevant parameters and the predicted, and experimental, spacings for the arsenides. We also give the contributions to the cohesion, all evaluated at the theoretically predicted  $d$ . We see that  $V_3(pf)$  goes through zero at uranium and that is where the predicted minimum is spacing occurs. We see in contrast that the contribution  $E_{pf \text{ bond}}$  to the cohesion continues to increase in magnitude through the series. This follows also from Eq. (8), which approaches  $12V_3$  as  $V_3$  becomes large and negative. (The final term is small.) It is just the derivative, Eq. (9), which becomes maximum when  $V_3$  is zero.

We have no experimental information concerning the cohesion and bulk modulus for these systems. The other cases we have considered in this paper suggest that the accuracy of the predictions would be low but that the trends found may be meaningful.

#### ACKNOWLEDGMENTS

This work was supported in part by the Los Alamos National Laboratories under the U.S. Department of Energy Contract No. W-7405-Eng-36 and in part by the National Science Foundation under Grant No. DMR-84 14126.

#### APPENDIX A: AVERAGE BAND ENERGIES FROM THE SECOND MOMENT

The electronic structure of the transition-metal compounds is represented by bands such as those of Fig. 1.

To obtain the total energy of the solid we needed a sum of energies over the lower set of three bands. We wish to obtain the sum approximately by calculating the second moment of the bands. This is conveniently formulated by writing each band state as a linear combination of the five  $d$  states on each of the  $N$  metal atoms and of the three  $p$  states on each of the  $N$  nonmetallic atoms. This leads to an  $8N \times 8N$  Hamiltonian matrix,  $H_{ij}$ . If the eigenvalues are written  $\epsilon_k$ , the second moment measured from  $(\epsilon_d + \epsilon_p)/2$  is

$$\langle \epsilon_k^2 \rangle = (1/8N) \sum_k \epsilon_k^2 = (1/8N) \sum_{ji} H_{ij} H_{ji}, \quad (\text{A1})$$

since the matrix  $H^2$  is Hermitian and diagonalizing it does not change the sum of its diagonal elements  $\epsilon_k^2$ . Since we measure eigenvalues from  $(\epsilon_p + \epsilon_d)/2$ , the diagonal terms are all  $V_3^2$ , with  $V_3 = (\epsilon_d - \epsilon_p)/2$ , contributing  $8NV_3^2$  to the sum. If we sum over states  $i$  on one metal atom, the sum over the  $j$  on neighboring nonmetal atoms will be independent of which metal atom we selected, and in fact the sum over  $i$  and the  $j$  on a single one of the  $n$  nonmetal neighbors will be the same for each neighbor. Thus,

$$\langle \epsilon_k^2 \rangle = (n/8) \sum_{i,j} 2H_{ij} H_{ji} + V_3^2, \quad (\text{A2})$$

where now  $i$  runs over states on one metal atom and  $j$  over states on one neighboring nonmetal atom. This sum is in fact  $2 \sum_m V_{pdm}^2$ ,  $m = -1$  to 1. A factor of 2 came from adding the terms with metal and nonmetal interchanged.  $8 \langle \epsilon_k^2 \rangle$  is the sum of the  $\epsilon_k^2$  over all eight bands. If we drop the two nonbonding bands at  $\epsilon_k = V_3$ , and divide by 6 to obtain the average of the remaining six we obtain

$$\langle \epsilon_k^2 \rangle_{\text{bond}} = (n/3) \sum_{m=-1}^1 V_{pdm}^2 + V_3^2. \quad (\text{A3})$$

The first term on the right is called the square of the covalent energy,  $[V_2(pd)]^2$ . For a general pair of bands based upon orbital angular momentum quantum numbers  $l$  and  $l'$  with  $l \leq l'$  the covalent energy is

$$(V_2^{ll'})^2 = [n/(2l+1)] \sum_{m=-l}^l V_{ll'm}^2, \quad (\text{A4})$$

with  $n$  again the number of nearest neighbors.

We take the average of the lower band energy to be

$$(\varepsilon_l + \varepsilon_{l'})/2 - \langle \varepsilon_k^2 \rangle^{1/2} = (\varepsilon_l + \varepsilon_{l'})/2 - (V_2^2 + V_3^2)^{1/2}.$$

We may verify by substituting Eq. (A4) for  $V_2^2$  that for small  $V_2$ , an expansion to second order gives exactly the result from second-order perturbation theory. It follows that if we are to use the form  $-(V_2^2 + V_3^2)^{1/2}$ , Eq. (A4) is the correct choice of  $V_2$ . The sum of energies over the  $2(2l+1)$  electrons (again  $l \leq l'$ ) per atom pair occupying these bonding bonds is

$$\sum_k \varepsilon_k = 2(2l+1)[(\varepsilon_l + \varepsilon_{l'})/2 - (V_2^2 + V_3^2)^{1/2}] \quad (\text{A5})$$

per atom pair. In computing cohesion, this would be subtracted from the sum over the  $\varepsilon_l$  and  $\varepsilon_{l'}$  for the atomic levels previously occupied by these electrons.

Simple compounds, such as NaCl, are a special case of this with  $l=0$ ,  $l'=1$ . Then

$$\sum_k \varepsilon_k = 2[(\varepsilon_p + \varepsilon_s)/2 - (V_2^2 + V_3^2)^{1/2}]$$

with  $V_2^2 = 6V_{sp\sigma}^2$  and  $V_3 = (\varepsilon_s - \varepsilon_p)/2$  as discussed above. This was derived earlier<sup>14</sup> using the Baldereschi special point method (described in Ref. 2). The result is now generalized to  $d$ - and  $f$ -shell systems though the generalization does not follow from the special points method.

In fact a form which may be more accurate than Eq. (A5) could be obtained by assuming a model density of states with a uniform density of states  $6/W_b$  in the bonding band of width  $W_b$  from  $(\varepsilon_l + \varepsilon_{l'})/2 - V_3$  to  $(\varepsilon_l + \varepsilon_{l'})/2 - V_3 - W_b$ . The same width is assumed for the antibonding band beginning  $2V_3$  above this, where the nonbonding band of zero width lies. We may calculate the  $\langle \varepsilon_k^2 \rangle$  for the bonding band with this density of states and equate it to Eq. (A3) to obtain an equation for  $W_b$

$$[(V_3 + W_b)^3 - V_3^3]/(3W_b) = V_2^2 + V_3^2. \quad (\text{A6})$$

This can be solved numerically and the average energy of the bonding band, obtained from the corresponding density of states, is  $-V_3 - W_b/2$ . The artificiality of the density of states did not seem to justify the added complexity. We took the simpler form  $-(V_2^2 + V_3^2)^{1/2}$ .

## APPENDIX B: DETERMINATION OF PARAMETERS

For  $sp$ -bonded systems we used universal tight-binding matrix elements<sup>8</sup> with  $V_{sp\sigma} = 1.42\hbar^2/md^2$ . For  $d$  and  $f$  shells we use Andersen's muffin-tin-orbital theory<sup>15</sup> as combined with transition-metal pseudopotentials<sup>16</sup> to obtain<sup>17</sup>

$$V_{ll'm} = (\eta_{ll'm}\hbar^2/m)[(r_l^{2l-1}r_{l'}^{2l'-1})^{1/2}/d^{l+l'+1}], \quad (\text{B1})$$

where  $r_l$  and  $r_{l'}$  are distances characteristic of the  $l$ th state of the free atom. Wills<sup>18</sup> has derived the general form for the coefficient

$$\eta_{ll'm} = \frac{(-1)^{l'+1}}{6\pi} \frac{(l+l')!(2l)!(2l')!}{2^{l+l'}l!l'!} (-1)^m \times \left[ \frac{(2l+1)(2l'+1)}{(l+m)!(l-m)!(l'+m)!(l'-m)!} \right]^{1/2}. \quad (\text{B2})$$

We will be interested here in couplings where  $l=1$ ,

$$\begin{aligned} \eta_{110} &= 1/\pi, & \eta_{111} &= -1/2\pi, \\ \eta_{120} &= -3\sqrt{15}/2\pi, & \eta_{121} &= 3\sqrt{5}/2\pi, \\ \eta_{130} &= 10\sqrt{21}/\pi, & \eta_{131} &= -15\sqrt{7}/2\pi. \end{aligned} \quad (\text{B3})$$

A procedure has been given<sup>17</sup> for obtaining  $r_l$  from the free-atom atomic state but a simpler and probably more reliable method is to obtain both the top and bottom of the pure metal bands from the atomic surface method<sup>19</sup> and choose  $r_l$  such that the tight-binding band width is the same. We already have  $r_d$  values and  $r_f$  values obtained in a similar way.<sup>19</sup> To obtain  $r_p$  we may put oxygen in a simple cubic structure and note that the maximum and minimum of the tight-binding  $p$  bands occur at  $k=(\pi/d, 0, 0)$  and are  $\pm(2V_{pp\sigma} - 4V_{pp\pi})$  corresponding to a band width [see Eq. (B3)] of

$$W_p = (8/\pi)\hbar^2 r_p / md^3. \quad (\text{B4})$$

It is interesting that precisely the same result is obtained [using again (B3)] for a body-centered-cubic structure for which the maximum and minimum appear to be, for example, states  $\pm|p_x\rangle$  on the cube corners and  $\pm|p_y\rangle$  on the cube centers.

In the atomic surface method the band width is given by<sup>19</sup>

$$W_p = -4\pi r_0^2 (\hbar^2/m) (\partial\rho_p/\partial r) |_{r_0} / \int_0^{r_0} 4\pi r^2 \rho_p dr, \quad (\text{B5})$$

where  $\rho_p$  is the angular average of the probability density for an atomic  $p$  state and  $r_0$  is the atomic sphere radius,  $4\pi r_0^3/3 = d^3$  for a simple cubic lattice. If Eq. (B5) gave a width varying exactly as  $d^{-3}$ , the  $r_p$  obtained from Eqs. (B4) and (B5) would not depend upon the choice of  $r_0$ . That will only be approximately true but we may choose an  $r_0$  such that  $\partial \ln W_p / \partial \ln r_0$  is approximately  $-3$ . We do this using the asymptotic form of the atomic wave function proportional to  $r^\nu e^{-\mu r}$  with  $\mu$  given by  $\varepsilon_p = -\hbar^2 \mu^2 / 2m$ . The exponent  $\nu$  is near zero and is dropped and the denominator in Eq. (B5) is near one and set equal to one. Then  $\partial\rho_p/\partial r = -2\mu\rho_p$  and  $\partial \ln W_p / \partial \ln r_0 = 2 - 2\mu r_0 = -3$  or  $\mu r_0 = \frac{5}{2}$ . For oxygen, with  $\varepsilon_p = -16.72$  eV this gives  $r_0 = 1.19$  Å or  $d = 1.92$  Å. Using Hartree-Fock wave functions and term values we have evaluated  $r_p$  from Eqs. (9) and (10) and listed them in Table V for the nonmetallic elements.

It may be useful also to do an approximate evaluation using the normalized asymptotic form  $\varepsilon_p = (\mu^3/\pi)e^{-2\mu r}$  and setting the denominator in Eq. (B5) equal to one. Then letting  $2\mu r_0 = 5$  we obtain

$$r_p \approx \pi^2 5^5 e^{-5} / 24\mu, \quad (\text{B6})$$

TABLE V. Tight-binding parameters for anion *p* states. The tight-binding parameter  $r_p$  for the anion *p* states as defined in Eq. (B1) in units of Å.

C	N	O
6.59	5.29	4.41
Si	P	S
13.7	11.4	10.1
Ge	As	Se
14.4	13.2	12.1
Sn	Sb	Te
18.0	16.8	15.9
Pb	Bi	Po
19.8	18.9	17.9

giving 4.13 Å for oxygen, in reasonable agreement with the more accurate value of 4.41 Å from Table V. We see that  $r_p$  varies inversely with the square root of  $|\epsilon_p|$ .

As a further test of our method we may evaluate

$$\begin{aligned} V_{pd\sigma} &= (-3\sqrt{15}/2\pi)(\hbar^2/m)(r_p r_d^3)^{1/2}/d^4, \\ V_{pd\pi} &= (3\sqrt{5}/2\pi)(\hbar^2/m)(r_p r_d^3)^{1/2}/d^4, \end{aligned} \quad (\text{B7})$$

for strontium titanate in the perovskite structure with  $d=1.95$  Å. For titanium  $r_d=1.08$  Å and we obtain from Eq. (B7)  $V_{pd\sigma}=-2.30$  eV and  $V_{pd\pi}=1.33$  eV in good accord with values  $-2.43$  and  $1.13$  eV obtained from a band calculation on SrTiO<sub>4</sub> by Mattheis.<sup>20</sup> Similar agreement is guaranteed for KTaO<sub>3</sub>, KMoO<sub>3</sub>, and ReO<sub>3</sub> since they differ only in  $r_d$  and the relative values were checked earlier.<sup>2</sup>

### APPENDIX C: THE OVERLAP REPULSION

The sum of the electronic energies in Eq. (A1) came from a Hermitian matrix, and therefore orthogonal orbitals. The average energy of all levels is then not shifted by the coupling. Real orbitals on neighboring atoms are not orthogonal and the overlap

$$S_{ll'm} = \int \psi_{lm}(\mathbf{r})\psi_{l'm}(\mathbf{r}-\mathbf{d})^3 \mathbf{r}, \quad (\text{C1})$$

causes an upward shift in the average energy and thus a repulsive "overlap interaction" between atoms. For *sp*-bonded ionic solids we used the virial theorem to suggest that this repulsion was given by<sup>1</sup>

$$V_0(d) = -\eta_0 \epsilon_{IG} [\hbar^2/(m \epsilon_{IG} d^2)]^4. \quad (\text{C2})$$

with  $\epsilon_{IG}$  the average of the *p*-state term value for the inert gas atom following the anion (Ne for O) and that for the inert gas atom preceding the cation (Ar for Ca). With this choice,  $\eta_0$  was found to depend only on the anion row, being given by 688 for the oxygen row, 1163 for the sulphur row, 1323 for the selenium row, and 1684 for the tellurium row. The combination of this repulsion and the bonding attraction stabilizes the structure. We shall use this same  $V_0$  for *d*- and *f*-state metal compounds but need to add the repulsion from the nonorthogonality of the *d* states and the neighboring anion *p* states.

The corresponding *d* bands are only partly occupied

and we must treat the repulsion in a different way. In particular we must see what the effect of nonorthogonality of neighboring orbitals is on the energy bands.

We begin with two coupled levels, such as the 1s states on two neighboring hydrogen atoms. We may form bonds as even and odd combinations of these two states and evaluate the energy as

$$\langle \psi | H | \psi \rangle / \langle \psi | \psi \rangle = \epsilon \pm \langle 1 | H | 2 \rangle / (1 \pm S),$$

where  $\epsilon_s = \langle 1 | H | 1 \rangle = \langle 2 | H | 2 \rangle$ , and  $S = \langle 1 | S = \langle 1 | 2 \rangle / \langle 2 | 2 \rangle$  is the nonorthogonality. The plus obtains for the bonding state (the coupling  $\langle 1 | H | 2 \rangle$  is negative) and the minus for the antibonding state. We define the covalent energy to be half the difference,  $V_2 = \langle 1 | H | 2 \rangle / (1 - S^2)$ , which is given by universal parameters. The shift in the average is then seen to be  $-SV_2$ , a positive shift, and the overlap repulsion is this shift times the number of electrons in these states. This same  $-SV_2$  is also correct even if there is a difference in energy between the two coupled states, a  $V_3$ .<sup>21</sup>

Similarly we may construct *pd* bands, as illustrated in Fig. 1. At each wave number each band consists of a linear combination of some *p* Bloch sum  $\sum_j \exp(i\mathbf{k}\cdot\mathbf{r}) | p_j \rangle$  and some *d* Bloch sum of the same wave number and we again evaluate  $\langle \psi | H | \psi \rangle / \langle \psi | \psi \rangle$ . If because of symmetry, as at  $k=0$  in Fig. 1, the two Bloch sums are uncoupled, we obtain simply the  $\epsilon_p$  or  $\epsilon_d$  with no shift due to coupling nor to nonorthogonality. For this symmetric case the two Bloch sums are also orthogonal, but at more general points in the zone where the Bloch sums are not orthogonal, there will be no shift  $-SV_2(\mathbf{k})$  when the coupling is zero. Thus the nonbonding bands are not shifted by the nonorthogonality and do not contribute to the overlap repulsion even when they are occupied. The average shift of bonding and antibonding bands is a direct generalization of the results for pure metals,<sup>17,18</sup> it is  $-1/(2l+1) \sum_m V_{ll'm} S_{ll'm}$  with the sum over  $-l \leq m \leq l$ . Again we have taken  $l \leq l'$ . As in the two-level case, one effect of the nonorthogonality is to modify the couplings which produce the bands [as for the  $V_2 = \langle 1 | H | 2 \rangle / (1 - S^2)$  in the two-level case]; this has already been taken into account by using universal matrix elements. The other is to provide an overlap repulsion equal to the sum of the number of electrons occupying the bonding and antibonding bands times the average shift of these bands,

$$\delta \bar{\epsilon} = -n / (2l+1) \sum_m V_{ll'm} S_{ll'm}. \quad (\text{C3})$$

Here we have also multiplied by the number of neighbors  $n$ , taking the shifts to be additive. Special cases of  $l=l'=2$  and  $l=l'=3$  were derived earlier.<sup>17,18</sup>

Wills<sup>18</sup> has derived formulas for the nonorthogonality

$$S_{ll'm} = \sigma_{ll'm} (r_l^{2l-1} r_{l'}^{2l'-1})^{1/2} / d^{l+l'-1} \quad (\text{C4})$$

with

$$\sigma_{ll'm} = -\frac{1}{2}(l+l')[1+(4m^2-1)/(2l-1)(2l'-1)]\eta_{ll'm}. \quad (\text{C5})$$

These may be substituted back into Eq. (C3) to give a

shift for  $pd$  coupling of

$$\delta\bar{\epsilon} = (15n/4\pi^2)(\hbar^2/m)r_p r_d^3/d^6, \quad (\text{C6})$$

and for  $pf$  coupling of

$$\delta\bar{\epsilon} = (175n/\pi^2)(\hbar^2/m)r_p r_f^5/d^8. \quad (\text{C7})$$

These are to be multiplied by the number of electrons per atom pair occupying the bonding and antibonding bands.

<sup>1</sup>W. A. Harrison, Phys. Rev. B **34**, 2787 (1986).

<sup>2</sup>W. A. Harrison, *Electronic Structure and the Properties of Solids* (Freeman, New York, 1980).

<sup>3</sup>D. G. Pettifor and R. Podloucky, Phys. Rev. Lett. **53**, 1080 (1984) (Structure determination).

<sup>4</sup>M. S. S. Brooks, J. Phys. F. **14**, 639 (1984); **14**, 653 (1984); **14**, 857 (1984) (Light-actinide compounds).

<sup>5</sup>J. Zaanen, G. A. Sawatzky, and J. W. Allen, Phys. Rev. Lett. **55**, 418 (1985) (Origin of band gaps).

<sup>6</sup>D. Damien and C. H. de Novion, J. Nucl. Mater. **100**, 167 (1981) (Actinides).

<sup>7</sup>J. B. Mann, Atomic Structure Calculations, 1: Hartree-Fock Energy Results for Elements Hydrogen to Lawrencium (unpublished), distributed by Clearinghouse for Technical Information, Springfield, Virginia 22151, listed also in *Electronic Structure and the Properties of Solids*, Ref. 2, p. 534.

<sup>8</sup>W. A. Harrison, Phys. Rev. B **24**, 5835 (1981).

<sup>9</sup>D. A. Papaconstantopoulos, W. E. Pickett, B. M. Klein, and L. L. Boyer, Phys. Rev. B **31**, 752 (1985).

<sup>10</sup> $r_d$  values are given in Ref. 2;  $r_p$  values are given in Table V here.

<sup>11</sup>W. A. Harrison, Phys. Rev. B **29**, 2917 (1984).

<sup>12</sup>S. Froyen, Phys. Rev. B **22**, 3119 (1980).

<sup>13</sup>There are irregularities in this sequence at europium and ytterbium near the center and the end in the series, respectively. These two elements, as free atoms and as metals, take an additional correlated  $f$  electron, leaving them chemically divalent rather than trivalent. They form  $AB$  compounds only with elements from the oxygen column. In these compounds they fill the oxygen shell, with the remaining electrons in  $f$  states. For europium compounds this leaves a spin of  $\frac{7}{2}$  and for ytterbium, a spin of zero. There is also a monoxide of samarium, valence 8, one to the left of europium. It then also is divalent in this compound, leaving a spin of 3.

<sup>14</sup>W. A. Harrison, Phys. Rev. B **23**, 5230 (1981).

<sup>15</sup>O. K. Andersen, Solid State Commun. **13**, 133 (1973).

<sup>16</sup>W. A. Harrison, Phys. Rev. **181**, 1036 (1969).

<sup>17</sup>W. A. Harrison, Phys. Rev. B **28**, 550 (1983).

<sup>18</sup>J. M. Wills and W. A. Harrison, Phys. Rev. B **28**, 4363 (1983).

<sup>19</sup>G. K. Straub and W. A. Harrison, Phys. Rev. B **31**, 7668 (1985).

<sup>20</sup>L. F. Mattheiss, Phys. Rev. B **6**, 4718 (1972).

<sup>21</sup>*Electronic Structure and the Properties of Solids*, Ref. 2, Appendix B.